Magnetizing Inductance Estimation Method of Induction Motor for EV Traction Considering Magnetic Saturation Changes According to Current and Slip Frequency

Du-Ha Park[1], Cheon-Ho Song[1], Yun-Jae Won[1], Jin-Cheol Park[2], Hyun-Su Kim[1], Ho-Ryul Park[1], Young-Doo Yoon[2], and Myung-Seop Lim[2]

[1]Department of Automotive Engineering (Automotive-Computer Convergence), Hanyang University, Seoul 04763, Republic of Korea
[2]Department of Automotive Engineering, Hanyang University, Seoul 04763, Republic of Korea

During the motor design stage, it is crucial to accurately predict the characteristics of the motor at various operating points. Performing finite-element analysis (FEA) for each point is time-consuming and impractical. Therefore, the motor parameters and losses are typically calculated for each load point and used to solve the voltage and torque equations, thereby reducing the time required for motor characteristic analysis. Thus, the accurate prediction of motor parameters is essential for optimizing the motor design. This study proposes a parameter estimation method for the design process of induction motors (IMs). Accordingly, the circuit parameters are estimated using a reduced amount of FEA data. A common approach for evaluating the circuit parameters of IMs is through locked-rotor and no-load tests. However, these methods have limitations, because they use a fixed frequency that may not be suitable for electric vehicle traction motors owing to their various driving points, high torque, and high power density. This article introduces an iterative method for estimating the magnetizing inductance in IMs, owing to its significant impact on torque. This method is based on the changes in saturation according to current and slip frequency.

Index Terms— **Circuit parameter, induction motor (IM), iterative method, magnetizing inductance, saturation, slip frequency.**

I. Introduction

OWING to their high coercivity and energy density, motors that use rare-earth permanent magnets (PMs) are widely used in various fields. However, because of the unstable supply of rare-earth PMs and their high prices, research on motors that do not use rare-earth PMs is being actively conducted. Among motors that do not use rare-earth materials, induction motors (IMs) are widely used by vehicle manufacturers because of their low cost, high robustness, low electromotive force under no-load conditions, low cogging torque, and low torque ripple [1], [2].

Industrial IMs are typically operated at rated speeds and current conditions with low torque density. However, high-power traction motors operate at various operating speeds and load conditions, with a higher torque density. Owing to variations in the saturation levels, the torque produced by an IM depends on the slip frequency and the ratio of the rotating magnetic-field speed to the rotor speed when the stator current is held constant [3]. Thus, to design IMs as traction motors, it is necessary to predict the motor characteristics under various slip conditions in addition to the current.

As conventional test methods for estimating the circuit parameters of an IM, the locked-rotor test and the no-load test described in the IEEE-115-2009 standard [4] have been widely used. Owing to the difficulty in conducting experiments under certain conditions, an alternative to conventional tests, the standstill frequency response test method, was developed in [5]. In addition, in [6], a method for estimating parameters using the nameplate and the Gauss–Seidel convergence method was proposed. In [7], a method was studied for estimating parameters using an optimal algorithm, such as particle swarm optimization. Despite these various approaches, a new parameter estimation method is required, because previous studies do not reflect the variation in equivalent circuit parameters according to the change in slip.

Therefore, this article proposes an iterative estimation method for the magnetizing inductance that considers changes in current and slip frequency. In the proposed method, the magnetizing inductance is modified based on the parameter estimation method of the IM using the locked-rotor and no-load tests described in IEEE standard 112-2004 [4]. It is modified using the difference between T_{ANA} and T_{FEA}, where T_{ANA} refers to the torque calculated analytically using the electric equivalent circuit and T_{FEA} denotes the torque calculated using finite-element analysis (FEA). The characteristics of IMs can be accurately predicted for a specific operating point using the proposed method.

II. Background

A. Concept of Slip in the IM

When an alternating current is directly applied to the stator windings of the IMs, currents are induced in the rotor bars owing to the difference in speed between the rotating magnetic field and the rotor. The interaction between the rotating magnetic field and the flux induced in the rotor bars makes the rotor rotate in the same direction as the rotating magnetic

Manuscript received 24 March 2024; revised 25 June 2024; accepted 2 July 2024. Date of publication 11 July 2024; date of current version 27 August 2024. Corresponding author: M.-S. Lim (e-mail: myungseop@hanyang.ac.kr).
Color versions of one or more figures in this article are available at https://doi.org/10.1109/TMAG.2024.3426663.
Digital Object Identifier 10.1109/TMAG.2024.3426663

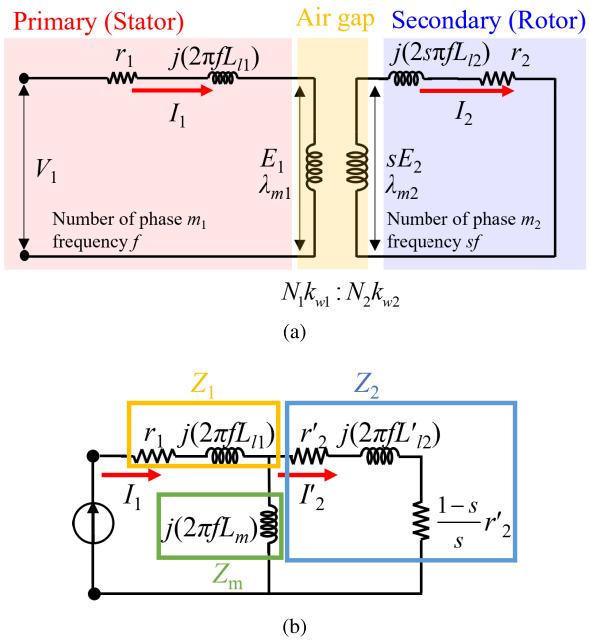

Fig. 1. Per-phase equivalent circuit of the IM. (a) Basic circuit. (b) Secondary side converted to primary side.

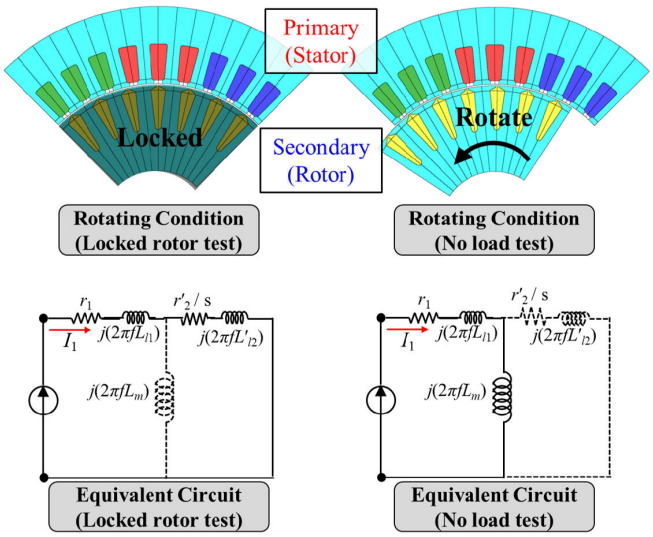

Fig. 2. Rotor rotating condition and the equivalent circuit of the locked-rotor test and the no-load test.

field under the Lorentz force. The unitized relative velocity of the rotating magnetic field and the rotor speed is called slip (s) and is defined in (1), where ω symbolizes the angular speed of rotating magnetic field and ω_m denotes the angular speed of rotor

$$s = \frac{\omega - \omega_m}{\omega}. \tag{1}$$

The frequency of the voltage induced in the rotor bars is called slip frequency (sf).

B. Equivalent Circuit of the IM

An equivalent circuit is used to predict the characteristics of IMs. Fig. 1 shows the per-phase equivalent circuit of an IM that does not reflect iron losses. The stator and rotor of the circuit are magnetically connected but electrically separated. The relationship between primary and secondary flux, induced electromotive force is defined in (2), where λ denotes the flux linkage, E denotes the induced electromotive force, N indicates the number of turns, and k_w is the winding factor

$$\lambda_{m1} = \frac{N_1 k_{w1}}{N_2 k_{w2}}\lambda_{m2}, \quad E_1 = \frac{N_1 k_{w1}}{N_2 k_{w2}}E_2. \tag{2}$$

The output power of the motor is generated from the air gap, so the torque can be calculated using (3), where $I'_{2\cdot\mathrm{rms}}$ refers to the root-mean-square value of the current flowing through the secondary part converted to primary, r'_2 is the secondary resistance converted to primary, and pp is the pole pair

$$T_{\mathrm{ANA}} = m_1 I'^2_{2\cdot\mathrm{rms}} \frac{r'_2}{s} \frac{1}{\omega_s \mathrm{pp}}. \tag{3}$$

C. Common Test Procedure of the IM

According to the IEEE standard test procedure for poly-phase IMs and generators, the circuit parameters of the IM can be obtained by measuring the stator winding resistance and performing the locked-rotor and no-load tests. First, the locked-rotor test provides information regarding the leakage inductance. If the rotor is constrained and cannot rotate, meaning the slip is one, the equivalent circuit of the IM under locked-rotor conditions can be represented, as shown in Fig. 2. The magnetizing reactance is generally much larger than the secondary resistance; therefore, the magnetizing current can be neglected. If the phase voltage, line current, and frequency measured at the stator terminal are known, the sum of the leakage reactance and secondary resistance can be obtained, as expressed in (4)–(7). Here, S_{LR} denotes the locked-rotor apparent power, P_{LR} denotes the locked-rotor active power, θ indicates the phase difference between phase voltage and line current, Z_{LR} indicates the locked-rotor impedance, R_{LR} denotes the locked-rotor resistance, X_{LR} denotes the locked-rotor reactance, x_{l1} denotes the primary leakage reactance, and x'_{l2} denotes the secondary leakage reactance converted to the primary

$$S_{\mathrm{LR}} = V_{1\cdot\mathrm{rms}} I_{1\cdot\mathrm{rms}}, \quad P_{\mathrm{LR}} = S_{\mathrm{LR}} \cos\theta \tag{4}$$

$$R_{\mathrm{LR}} = \frac{P_{\mathrm{LR}}}{I^2_{1\cdot\mathrm{rms}}}, \quad Z_{\mathrm{LR}} = \frac{V_{1\cdot\mathrm{rms}}}{I_{1\cdot\mathrm{rms}}} \tag{5}$$

$$X'_{\mathrm{LR}} = \sqrt{Z^2_{\mathrm{LR}} - R^2_{\mathrm{LR}}} \tag{6}$$

$$X_{\mathrm{LR}} = \frac{f_{\mathrm{rated}}}{f_{\mathrm{test}}} X'_{\mathrm{LR}} = 4X'_{\mathrm{LR}} = x_{l1} + x'_{l2}. \tag{7}$$

In addition, magnetizing inductance was calculated by performing a no-load test. Because the slip is close to zero in the no-load conditions, the rotor resistance, (r'_2/s), becomes very large, so the secondary current can be neglected. The equivalent circuit of the IM under no-load conditions is shown in Fig. 2. Similar to the previous locked-rotor test, the magnetizing reactance can be calculated, using the phase voltage, line current, and frequency measured at the stator terminal, as expressed in (8)–(11). Here, S_{NL} denotes the no-load apparent power, P_{NL} denotes the no-load active power,

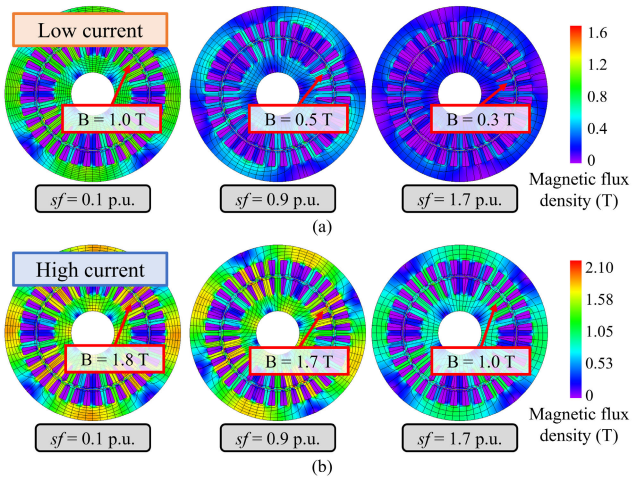

Fig. 3. Magnetic flux density distribution with the slip frequency changes under (a) low- and (b) high-current conditions.

θ denotes the phase difference between the phase voltage and the line current, Z_{NL} denotes the no-load impedance, R_{NL} denotes the no-load resistance, X_{NL} denotes the no-load reactance, and x_m denotes the magnetizing reactance

$$S_{\mathrm{NL}} = V_{1\cdot\mathrm{rms}} I_{1\cdot\mathrm{rms}}, \quad P_{\mathrm{NL}} = S_{\mathrm{NL}} \cos\theta \tag{8}$$

$$R_{\mathrm{NL}} = \frac{P_{\mathrm{NL}}}{I_{1\cdot\mathrm{rms}}^2}, \quad Z_{\mathrm{NL}} = \frac{V_{1\cdot\mathrm{rms}}}{I_{1\cdot\mathrm{rms}}} \tag{9}$$

$$X_{\mathrm{NL}} = \sqrt{Z_{\mathrm{NL}}^2 - R_{\mathrm{NL}}^2} \tag{10}$$

$$x_m = X_{\mathrm{NL}} - x_{l1}. \tag{11}$$

III. Proposed Method for Parameter Estimation

Following the IEEE standard [4], the circuit parameters of the IM can be obtained by measuring the stator winding resistance by performing locked-rotor and no-load tests. This testing method is applicable for industrial IMs with a small number of rated operating points. However, for traction IMs that operate over a wide driving area, the circuit parameters at different saturations must be considered to accurately predict the dynamic performance of the IM [8]. As shown in Fig. 3, even when the same current is applied, the magnetic saturation varies with slip frequency. Therefore, the change in the electric equivalent circuit parameter should be considered in response to both changes in current and slip-frequency variations.

A. Effect of Change in Parameters

To make accurate predictions, it is necessary to know how the torque is affected by the changes in each circuit parameter caused by various slips. When the stator current, slip frequency, and rotor speed are fixed, circuit parameters, such as L_{l1}, L_{l2}, L_m, and r_2, can be obtained using FEA, where L_{l1} and L_{l2} are the stator and rotor leakage inductances, respectively, L_m indicates the magnetizing inductance, and r_2 denotes the rotor resistance. Using these parameters, the torque can be calculated analytically using an electric equivalent circuit. Among these parameters, r_2 can be calculated directly by load analysis; therefore, only inductance was considered.

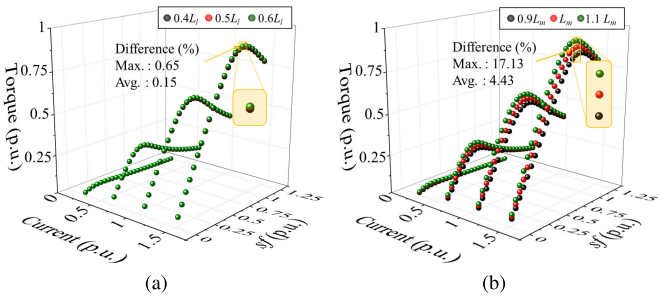

Fig. 4. Torque calculated by estimated parameters. (a) Considering leakage inductance split ratio changing from 0.4 to 0.6. (b) Considering magnetizing inductance changing from $0.9L_m$ to $1.1L_m$.

Fig. 4 illustrates how the torque changes when the leakage and magnetizing inductances change.

Since the estimation process for each parameter is different, the range of variation was set accordingly. The leakage inductance was compared with a split ratio of 0.4–0.6, considering the IEEE standard [4], while the magnetizing inductance was compared with the change in the result value of 0.9–1.1 times, effectively resulting in a $\pm 10\%$ variation range for the magnetizing inductance and a $\pm 20\%$ variation range for the leakage inductance. This confirms that the leakage inductance has a larger variation range. As shown in Fig. 4, the magnetizing inductance has a greater impact on the torque variation than the leakage inductance because of the smaller variation range in the magnetizing inductance resulted in greater torque variation. Therefore, it is crucial to predict the magnetizing inductance accurately.

B. Modification Method of the Magnetizing Inductance

Upon obtaining the current representative parameters from previous tests, the magnetizing inductance for the slip is modified using the differences between T_{ANA} and T_{FEA} according to the following steps.

1) *Step 1:* Select load points (I_1 and sf).
2) *Step 2:* Perform common test procedure described in Section II using FEA to calculate L_{l1}, L_{l2}, and L_m.
3) *Step 3:* Perform load analysis using FEA to obtain T_{FEA} and r_2.
4) *Step 4:* Calculate T_{ANA} using calculated parameters.
5) *Step 5:* Calculate the error between T_{ANA} and T_{FEA} for the corresponding load points.
6) *Step 6:* If the absolute error is greater than its reference value, the magnetizing inductance is modified using the product of the error and the adjustment rate. Update the iterative number and magnetizing inductance, and return to Step 4.
7) *Step 7:* If the absolute error is smaller than the reference value, the process is considered complete.

The flowchart of the process is shown in Fig. 5.

The results of modifying the magnetizing inductance using this process are presented in Fig. 6. Based on these results, the secondary current and torque before and after the magnetizing inductance modification were calculated and compared with the FEA results. As shown in Fig. 7, the proposed method

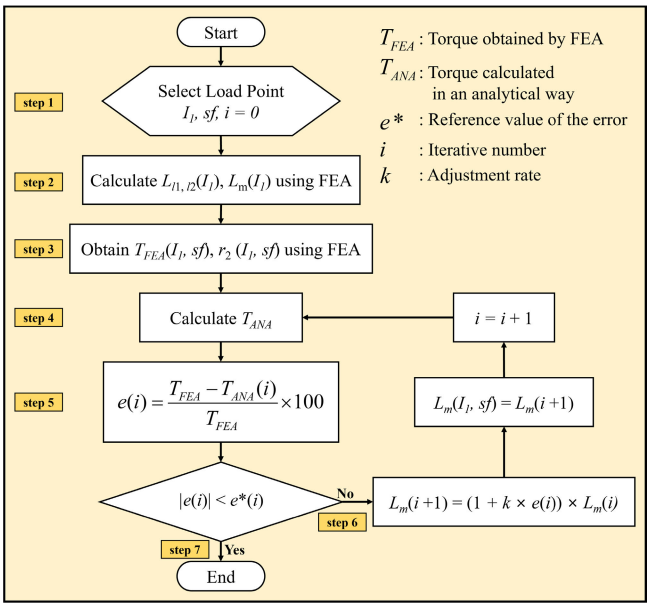

Fig. 5. Flowchart of the magnetizing inductance modification method.

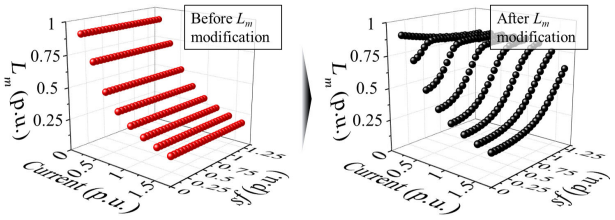

Fig. 6. Comparison of the magnetizing inductance before and after modification.

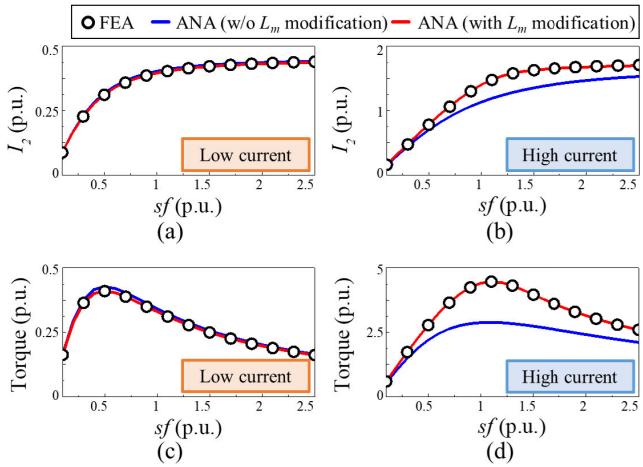

Fig. 7. Comparison of the rotor bar current using FEA and analytical approaches (without or with magnetizing inductance modification) under (a) low- and (b) high-current conditions. Comparison of T_{FEA} and T_{ANA} (without or with magnetizing inductance modification) under (c) low- and (d) high-current conditions.

was confirmed to be more useful when the difference in the saturation with the change in the slip frequency is large.

IV. Experimental Verification

This section presents a comparison between the FEA and experimental results. For experimental verification, a test

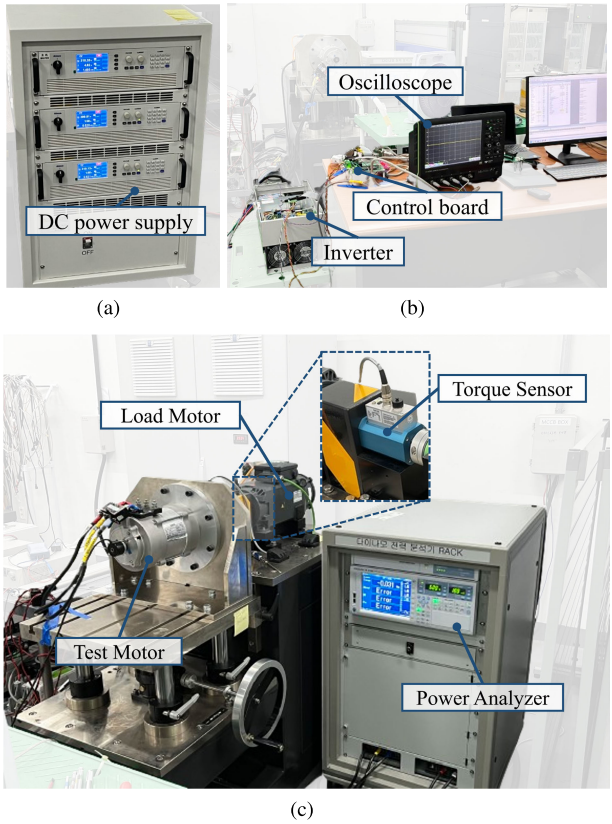

Fig. 8. Test configuration. (a) DC power supply. (b) Inverter, control board, and oscilloscope. (c) Test motor, load motor, torque sensor, and power analyzer.

TABLE I
Specifications of IM

Item	Unit	Value
Pole	-	4
Slot	-	36
Number of rotor bars	-	28
Output power	kW	3.5
DC voltage	V_{DC}	60
Frequency	Hz	102
Rated current	A_{rms}	72
Rated speed	rpm	3000
Core material	-	50PN470
Rotor bar material	-	aluminum

configuration for the IM was constructed, as shown in Fig. 8. The specifications of the IM used in the test are shown in Table I. The test was conducted by measuring the friction torque of the motor in the no-load test and the load torque of the motor in the load test.

In the load test, the measured torque would have been reduced by the friction torque generated by the mechanical friction of the motor. However, this friction torque is not included in T_{FEA} and T_{ANA}. Therefore, a no-load test was conducted to measure the friction torque at the corresponding speed. The friction torque obtained in this manner was subsequently incorporated into (12) to calculate T_{test}, where T_{test} denotes the load test torque considering friction, T_{load} denotes

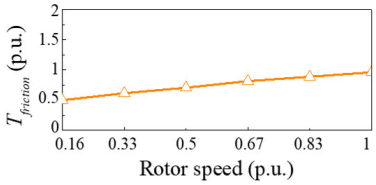

Fig. 9. Friction torque obtained from no-load test.

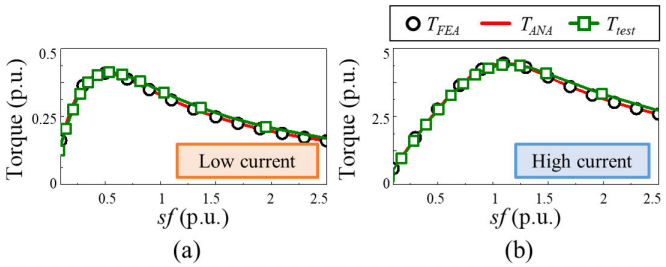

Fig. 10. Load torque obtained from load test under (a) low- and (b) high-current conditions.

the torque obtained from the load test, and T_{friction} denotes the friction torque obtained from the no-load test

$$T_{\text{test}} = T_{\text{load}} + T_{\text{friction}}. \tag{12}$$

A no-load test was conducted by driving the load motor at the rated speed, and T_{test} was measured at various rotor speeds, as shown in Fig. 9. The load test was conducted by controlling the current and frequency of the test motor using the indirect vector control method with an inverter and control board, as shown in Fig. 8(b), while the load motor was speed controlled at the rated speed. T_{load} was measured under various sf conditions, as shown in Fig. 10(a) and (b). Under low- and high-current conditions, the maximum error between T_{test} and T_{ANA} is 0.12% and 1.05%, respectively, which is within the acceptable range.

V. Conclusion

This article proposed an iterative method for estimating the magnetizing inductance of IMs by considering the changes in the current and slip frequency. The purpose of this parameter estimation method is to apply it during the design stage of the motor. Although it requires FEA data and take some time to complete the analysis, it offers the advantage of estimating parameters without the need for experimental results. In the design process of IMs for traction applications, it is essential to consider both the current and slip frequency owing to their various operating points. The existing parameter estimation methods only provide a representative value of the current, necessitating a new approach. The proposed method modified the magnetizing inductance by using the difference between T_{FEA} and T_{ANA}. This approach is expected to reflect the magnetic saturation changes owing to different operating conditions of the IMs in the magnetizing inductance. Finally, the proposed method was experimentally verified through no-load and load tests, thereby confirming its effectiveness and accuracy.

Acknowledgment

This work was supported by the Korea Institute of Energy Technology Evaluation and Planning (KETEP) Grant funded by the Korea Government (MOTIE) through the Development of Common Base Technology for Medium Power Industrial Motors under Grant RS-2023-00232593.

References

[1] B. Poudel, E. Amiri, P. Rastgoufard, and B. Mirafzal, "Toward less rare-earth permanent magnet in electric machines: A review," *IEEE Trans. Magn.*, vol. 57, no. 9, pp. 1–19, Sep. 2021.

[2] L. Shao, A. E. H. Karci, D. Tavernini, A. Sorniotti, and M. Cheng, "Design approaches and control strategies for energy-efficient electric machines for electric vehicles—A review," *IEEE Access*, vol. 8, pp. 116900–116913, 2020.

[3] L. Monjo, F. Córcoles, and J. Pedra, "Saturation effects on torque- and current–slip curves of squirrel-cage induction motors," *IEEE Trans. Energy Convers.*, vol. 28, no. 1, pp. 243–254, Mar. 2013.

[4] *IEEE Standard Test Procedure for Polyphase Induction Motors and Generators*, Standard IEEE Std 112-2004 (Revision IEEE Std 112-1996), 2004, pp. 1–83.

[5] A. Belqorchi, U. Karaagac, J. Mahseredjian, and I. Kamwa, "Standstill frequency response test and validation of a large hydrogenerator," *IEEE Trans. Power Syst.*, vol. 34, no. 3, pp. 2261–2269, May 2019.

[6] K. Lee, S. Frank, P. K. Sen, L. G. Polese, M. Alahmad, and C. Waters, "Estimation of induction motor equivalent circuit parameters from nameplate data," in *Proc. North Amer. Power Symp. (NAPS)*, Sep. 2012, pp. 1–6.

[7] D. Bhowmick, M. Manna, and S. K. Chowdhury, "Estimation of equivalent circuit parameters of transformer and induction motor from load data," *IEEE Trans. Ind. Appl.*, vol. 54, no. 3, pp. 2784–2791, May 2018.

[8] M. A. Masadeh, K. S. Amitkumar, and P. Pillay, "Power electronic converter-based induction motor emulator including main and leakage flux saturation," *IEEE Trans. Transport. Electrific.*, vol. 4, no. 2, pp. 483–493, Jun. 2018.